Scientific Journal of Silesian University of Technology. Series Transport
Zeszyty Naukowe Politechniki Śląskiej. Seria Transport

Volume 130 **2026**

p-ISSN: 0209-3324

e-ISSN: 2450-1549

DOI: https://doi.org/10.20858/sjsutst.2026.130.4

Journal homepage: http://sjsutst.polsl.pl

Article citation information:
Chríbik, A., Luknár, L. Combustion characteristics of high-energy syngas in internal combustion engines under constant CO_2 and N_2 conditions. *Scientific Journal of Silesian University of Technology. Series Transport*. 2026, **130**, 65-76. ISSN: 0209-3324. DOI: https://doi.org/10.20858/sjsutst.2026.130.4

Andrej CHRÍBIK[1], Lukáš LUKNÁR[2]

COMBUSTION CHARACTERISTICS OF HIGH-ENERGY SYNGAS IN INTERNAL COMBUSTION ENGINES UNDER CONSTANT CO_2 AND N_2 CONDITIONS

Summary. Within the framework of promoting circular economy strategies and expanding the portfolio of renewable energy sources, synthesis gases (syngas) produced from the gasification of municipal and plastic waste constitute a promising alternative fuel. This research investigates five high-energy syngas compositions, each maintaining constant inert gas proportions (10% CO_2 and 5% N_2), focusing on their combustion behavior in a spark-ignition internal combustion engine designed for cogeneration applications. This analysis focuses on the characterization of in-cylinder pressures, the indicated mean effective pressure (IMEP), heat release dynamics, and the duration of the combustion process. Experimental results demonstrate that elevated hydrogen proportion in fuel mixtures accelerates combustion, evidenced by reduced burn duration. However, hydrogen content did not exhibit a direct correlation with peak in-cylinder pressure. The maximum peak pressure was achieved by a mixture containing moderate hydrogen and elevated carbon monoxide content. A hydrogen-rich mixture displayed the shortest burn duration yet produced the lowest maximum pressure, attributed to spark timing positioned near top dead center (TDC). Methane

[1] Faculty of Mechanical Engineering, The Slovak University of Technology in Bratislava, Námestie Slobody17, 812-31 Bratislava, Slovakia. Email: andrej.chribik@stuba.sk. ORCID: https://orcid.org/0000-0001-7513-2786
[2] Faculty of Mechanical Engineering, The Slovak University of Technology in Bratislava, Námestie Slobody17, 812-31 Bratislava, Slovakia. Email: lukas.luknar@stuba.sk. ORCID: https://orcid.org/0009-0000-1142-6152

concentration directly influenced the volumetric lower heating value (LHV), subsequently affecting both IMEP and torque output. Relative to methane operation, engine torque output decreased by 6% to 13.4%, while hourly fuel consumption increased from 1.55 kg.h^{-1} to 3.88 kg.h^{-1} depending on mixture composition.

Keywords: syngas from wastes, internal combustion engine, renewable energy from waste

1. RESEARCH CONTEXT

The advancement of sustainable energy technologies has catalyzed significant research in thermochemical waste conversion methods, particularly within circular economy frameworks. Market projections indicate that the waste-to-energy sector was valued at USD 42.5 billion in 2024, with anticipated growth to USD 68.0 billion by 2030, representing a compound annual growth rate of 8.3% [1]. This expansion reflects the convergence of rising energy demand, increasingly restrictive environmental legislation, and alignment with United Nations Sustainable Development Goals targeting carbon neutrality [2].

Municipal solid waste (MSW) generation exhibits a persistent upward trajectory globally, with forecasts suggesting an increase to 3.4 billion metric tons annually by 2050 [3]. Data from the central European region demonstrate particularly pronounced growth trends, with per capita waste production in the Slovak Republic, the Czech Republic, Hungary, the Republic of Poland and Republic of Austria showing consistent increases over three decades [4].

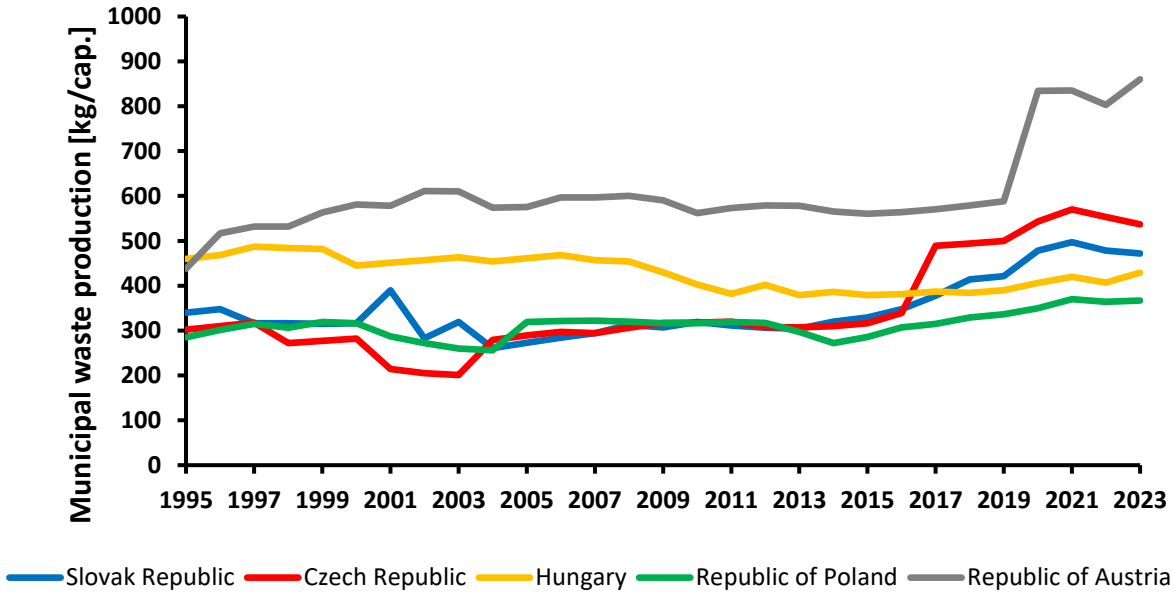

Fig. 1. Per capita municipal waste generation trends in Central Europe [4]

Conventional waste management methodologies, predominantly landfilling and direct thermal treatment, prove increasingly inadequate due to environmental burden and limited resource valorization potential [5]. Among advanced thermochemical conversion technologies, gasification processes have demonstrated superior potential for MSW treatment.

This technology operates through controlled partial oxidation at elevated temperatures with sub-stoichiometric oxygen supply, yielding synthesis gas – a combustible gaseous mixture containing methane (CH_4), hydrogen (H_2), carbon monoxide (CO), with inevitable inert components including carbon dioxide (CO_2) and nitrogen (N_2) [6, 7]. Contemporary technological developments in gasification systems, including enhanced updraft reactor configurations and plasma-assisted gasification, have achieved improved energy recovery efficiencies while minimizing pollutant emissions relative to conventional combustion approaches [8, 9].

Utilization of synthesis gases in spark-ignition internal combustion engines (ICE) for combined heat and power (CHP) applications represents a technically viable pathway for distributed energy generation, particularly in small to medium-scale installations. Experimental investigations have confirmed that syngas-fueled ICEs can achieve performance characteristics comparable to natural gas operation while simultaneously contributing to waste volume reduction and fossil fuel displacement [10, 11]. Nevertheless, compositional variability of waste-derived syngas, influenced by feedstock heterogeneity and gasification operational parameters, presents significant challenges for engine calibration and operational stability [12, 13].

The physicochemical characteristics of syngas deviate substantially from conventional gaseous fuels. Hydrogen content enhances flame propagation kinetics and extends flammability limits, facilitating lean combustion strategies with potential thermal efficiency improvements [14, 15]. Conversely, carbon monoxide presence and inert gas dilution affect volumetric lower heating value (LHV), consequently influencing engine power output and specific fuel consumption [16]. A comprehensive understanding of specific syngas compositional effects on combustion behavior, particularly under conditions representative of waste-derived gases with standardized inert content, remains essential for gasification-engine integrated system optimization.

Contemporary systematic reviews emphasize the necessity for detailed investigation of syngas combustion characteristics in ICEs, highlighting knowledge gaps regarding constant inert gas content influence on engine performance parameters [17, 18]. While substantial research has examined syngas utilization in dual-fuel configurations across various H_2/CO ratios, systematic analysis of fixed CO_2 and N_2 proportions across different H_2, CO, and CH_4 combinations remains limited – a scenario particularly relevant to controlled gasification processes targeting specific inert gas concentrations for operational stability [19, 20].

This experimental investigation addresses this research gap through examination of five distinct high-energy syngas compositions, each formulated with constant carbon dioxide (10% vol.) and nitrogen (5% vol.) proportions, representative of typical waste gasification outputs following preliminary cleaning processes. The research focuses on a spark-ignition internal combustion engine operating at rated speed conditions appropriate for cogeneration applications. Key combustion parameters, including in-cylinder pressure evolution, indicated mean effective pressure (IMEP), heat release characteristics, and combustion duration, are systematically analyzed to elucidate the influence of varying H_2, CO, and CH_4 content on engine operational behavior.

Research outcomes provide practical guidance for configuring waste gasification technologies to achieve optimal syngas composition for ICE-based CHP systems, thereby contributing to development of economically viable and environmentally sustainable waste-to-energy solutions.

The present investigation explores the operational impact of specific gaseous fuel mixtures on a reciprocating internal combustion engine. The chosen fuels simulate syngas compositions generated through municipal waste and plastic gasification, thereby supporting the determination of favorable compositional limits for syngas use. Table 1 provides the relevant fuel characteristics, and Figure 2 graphically displays their compositional profiles.

Tab. 1

Fundamental properties of the selected syngas mixtures

Parameter	Unit	Methane	SG1	SG2	SG3	SG4	SG5
N_2	[% vol.]	0	5	5	5	5	5
CO_2	[% vol.]	0	10	10	10	10	10
CO	[% vol.]	0	25	35	35	25	30
H_2	[% vol.]	0	40	30	10	30	20
CH_4	[% vol.]	100	20	20	40	30	35
Lower heating value	[MJ.kg^{-1}]	50.011	19.495	17.095	19.988	21.074	20.474
$LHV_{mixture}$	[MJ.kg^{-1}]	2.762	2.817	2.789	2.726	2.772	2.743
Lower heating value	[MJ.m^{-3}]	33.354	13.631	13.799	18.467	15.964	17.213
$LHV_{mixture}$	[MJ.m^{-3}]	3.172	3.064	3.100	3.145	3.090	3.115
Molar mass	[kg.kmol^{-1}]	16.0	16.8	19.4	22.2	18.2	20.2
$\rho_{NTP\ fuel}$	[kg.m^{-3}]	0.667	0.699	0807	0.924	0.758	0.841
Mixture composition	[kg.kg^{-1}]	17.1	5.9	5.1	6.3	6.6	6.5
Fuel in air	[% vol.]	9.5	22.5	22.5	17.0	19.4	18.1
$\rho_{NTP\ mixture}$	[kg.m^{-3}]	1.152	1.091	1.115	1.157	1.118	1.139

*LHV – lower heating value, NTP – normal temperature and pressure

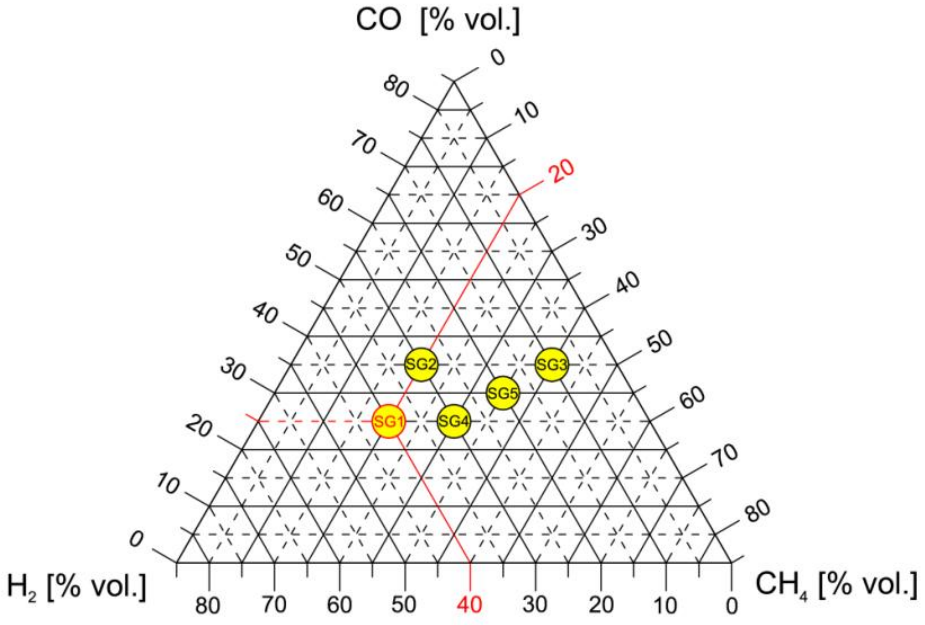

Fig. 2. Ternary diagram of selected syngas compositions with constant inert gas quantities (10% vol. CO_2, 5% vol. N_2), highlighting example syngas SG1 composition (20% vol. CH_4, 40% vol. H_2, 25% vol. CO)

2. EXPERIMENTAL METHODOLOGY

The effects of the selected gaseous fuels on the combustion characteristics were thoroughly investigated using a four-stroke, spark-ignition engine operating at atmospheric conditions, specifically the Lombardini LGW 702 model. This two-cylinder engine has a total displacement of 686 cm³, a compression ratio of 12.5:1, and a crankshaft with a 180° phase separation. The air–fuel mixture was generated using a mixing unit equipped with a diffuser, and the mixture's equivalence ratio was accurately regulated through a wideband lambda sensor integrated within a closed-loop control system. A schematic representation of the experimental engine setup is provided in Figure 3.

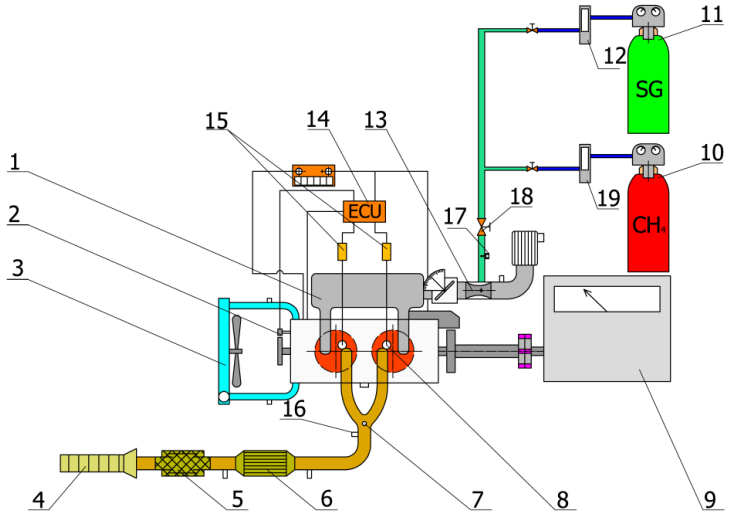

Fig. 3. Schematic depiction of the LGW 702 engine, illustrating the arrangement and identification of its principal components. (1 - Air intake manifold, 2 - Engine crank angle sensor, 3 - Coolant radiator, 4 - Exhaust manifold, 5 - Muffler, 6 - Three-way catalytic converter, 7 - Exhaust gas monitoring sensor for temperature and pressure, 8 - In-cylinder pressure sensor integrated into spark plug, 9 - Engine dynamometer (inductive type), 10 - Compressed methane cylinder, 11 - Compressed syngas cylinder, 12, 19 - Mass flow meters for gases, 13 - Fuel-air mixing device with integrated diffuser, 14 - Electronic control unit (ECU), 15 - Spark ignition coil, 16 - Wideband oxygen sensor, 17 - Incremental rotary motor,18 - System for regulating air-fuel mixture)

For this study, the selected engine served as the prime mover for a compact cogeneration system. Consequently, the investigation concentrated on the engine's rated speed of 1 500 min^{-1}. At this operating point, the spark ignition timing was systematically varied to identify the optimal advance angle under stoichiometric conditions at full load for each tested gaseous fuel. The optimization of the advanced ignition angle was performed with the aim of achieving the maximum indicated mean effective pressure during stable engine operation. The analysis focused primarily on key combustion characteristics, including in-cylinder pressure evolution, indicated mean effective pressure (IMEP), and the fuel mass fraction burned (MFB). These parameters were obtained from in-cylinder pressure measurements recorded using a Kistler spark plug featuring an embedded pressure sensor. Data processing was carried out using a custom-developed Matlab tool, which applies a single-zone, zero-dimensional thermodynamic model founded on the first law of thermodynamics for a closed system.

The heat release rate was evaluated employing the Rassweiler-Withrow method to accurately characterize combustion dynamics. It should be noted that all experiments were conducted at a single operating point corresponding to rated engine speed (1500 min^{-1}), full load, and stoichiometric air–fuel ratio. This approach was intentionally selected to represent the typical steady-state operation of small-scale cogeneration units. However, such a limitation restricts the general applicability of the findings to other engine operating regimes, such as part-load conditions, lean-burn strategies, or variable speed operation. Combustion behavior, pressure development, and IMEP trends may differ under those conditions due to changes in turbulence intensity, residual gas fraction, and heat transfer characteristics. Therefore, the presented results should be interpreted primarily within the context of rated steady-state operation.

Furthermore, the ignition timing was individually optimized for each tested fuel in order to achieve maximum IMEP under stable operating conditions. While this procedure ensures thermodynamically optimal combustion phasing for each mixture, it partially influences the direct comparability of peak pressure levels and pressure rise rates between fuels. Differences in combustion phasing may therefore reflect both intrinsic fuel reactivity and the adjusted spark timing strategy.

3. RESULTS AND DISCUSSION

The combustion process was evaluated using in-cylinder pressure analysis. As illustrated in Figure 4, the curves depict the averaged in-cylinder pressures obtained from 195 consecutive engine cycles for each tested gaseous fuel, operating under stoichiometric mixture conditions, optimal ignition timing, full load, and an engine speed of 1500 min^{-1}.

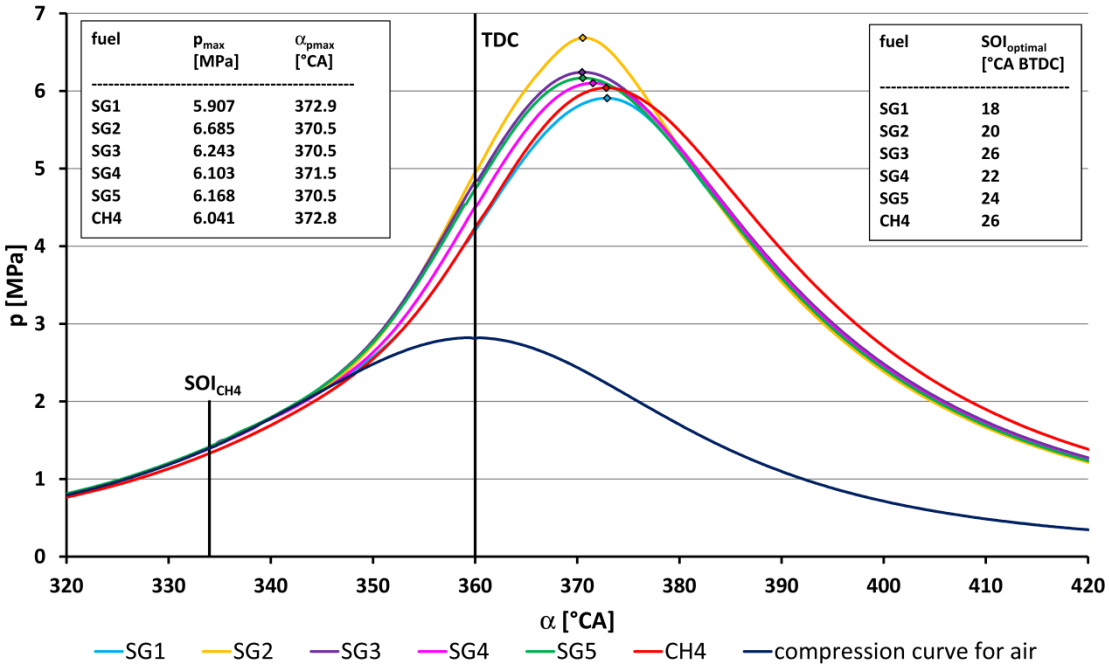

Fig. 4. In-cylinder pressure development during combustion. Experimental conditions: engine speed 1500 min^{-1}, stoichiometric air–fuel ratio, full load, and optimal ignition timing for each type of fuel

Because the ignition timing was optimized individually for each gaseous mixture, the observed differences in peak pressure position and magnitude cannot be attributed solely to compositional effects. Instead, they represent a combined outcome of fuel chemical kinetics and adjusted combustion phasing. This aspect is particularly relevant when comparing hydrogen-rich mixtures, where faster flame propagation required spark timing closer to TDC to prevent excessive pressure rise during the compression stroke. As shown in Figure 4, the syngas labeled SG2 reached the highest peak pressure during combustion, approximately 6.7 MPa, occurring near top dead center (TDC) at 10.5° crank angle (CA) after TDC. This is primarily attributed to SG2's shortest combustion duration ($\alpha_{10–90MFB}$) among all tested gases, as shown in Figure 5 below. In contrast, the lowest peak pressure was observed with SG1 syngas, around 5.9 MPa, at 12.9°CA after TDC. Interestingly, this phenomenon cannot be explained by variations in the combustion period, as the combustion duration of SG1 was similar to that of SG2, as shown in Figure 5. This finding is particularly notable considering SG1 contained the highest share of fast-burning hydrogen (40% vol.) among all syngases tested. Furthermore, the highest indicated mean effective pressure (IMEP) was recorded for start of ignition (SOI) timings at 16°CA and 18°CA before TDC, closer to TDC than for any other syngas, which likely influenced both the relatively low peak pressure and its delayed timing. Other syngases produced only slightly higher maximum combustion pressures compared to methane (ranging from 6.10 to 6.24 MPa versus 6.04 MPa), with peak pressures occurring marginally closer to TDC (10.5°-11.5°CA after TDC versus 12.8°CA after TDC for CH_4).

The peak rates of pressure increase for most of the tested fuels were slightly higher than those observed for the reference fuel, methane (0.225 MPa/°CA), ranging from 0.230 MPa/°CA for SG2 up to 0.240 MPa/°CA for SG3. The only exception was SG1, which reached only 0.195 MPa/°CA. This result is somewhat surprising, as the fuel with the highest hydrogen content exhibited the lowest pressure rise rate, while the fuel with the lowest hydrogen fraction showed the highest rate.

The combustion traces shown in Figure 5 reveal that each of the tested gaseous mixtures exhibited faster burn rates compared to the stoichiometric methane mixture, which reached a combustion duration of 24.4°CA. Among them, syngas SG3 exhibited the longest $\alpha_{10–90\ MFB}$ duration at 23.4°CA, while gases SG1 and SG2 shared the shortest value of 19.5°CA. The slower combustion of SG3 was anticipated, as its composition includes the lowest hydrogen content (10 vol.%) together with the highest carbon monoxide (35 vol.%) and methane (40 vol.%) fractions. Conversely, the mixture SG1, with the largest hydrogen fraction of 40 vol.%, showed the shortest burn time, consistent with expectations.

Although peak in-cylinder pressure and fuel burnout rates can indicate the effect of a given fuel on brake torque, the Indicated Mean Effective Pressure represents a more reliable metric for quantifying this influence. Figure 6 shows the IMEP values for all tested fuels and ignition timings, with the data points indicated by dots.

At the optimal ignition timing, the highest mean IMEP was recorded for pure methane, reaching 0.965 MPa, followed by syngas SG3 with an IMEP of 0.903 MPa. The results in Figure 6 indicate that combustion of SG5 was associated with significant IMEP fluctuations, suggesting potential instability in engine operation. The coefficient of variation (COV) for SG5 at the optimal ignition timing was 2.91%, nearly six times higher than that of SG2 (0.55%) and almost twice the second-highest value observed for SG1 (1.71%).

The third-highest Indicated Mean Effective Pressure was observed for SG4 (0.868 MPa), with SG2 (0.865 MPa), SG1 (0.861 MPa), and SG5 (0.860 MPa) trailing in close succession. Interestingly, although SG5 exhibited the lowest average IMEP, it generated the third-highest output torque, surpassed only by methane and SG3; however, its torque also displayed notable

fluctuations. Compared to the methane operation, the output torque decreased by 6% for SG3 and by up to 13.4% for SG1.

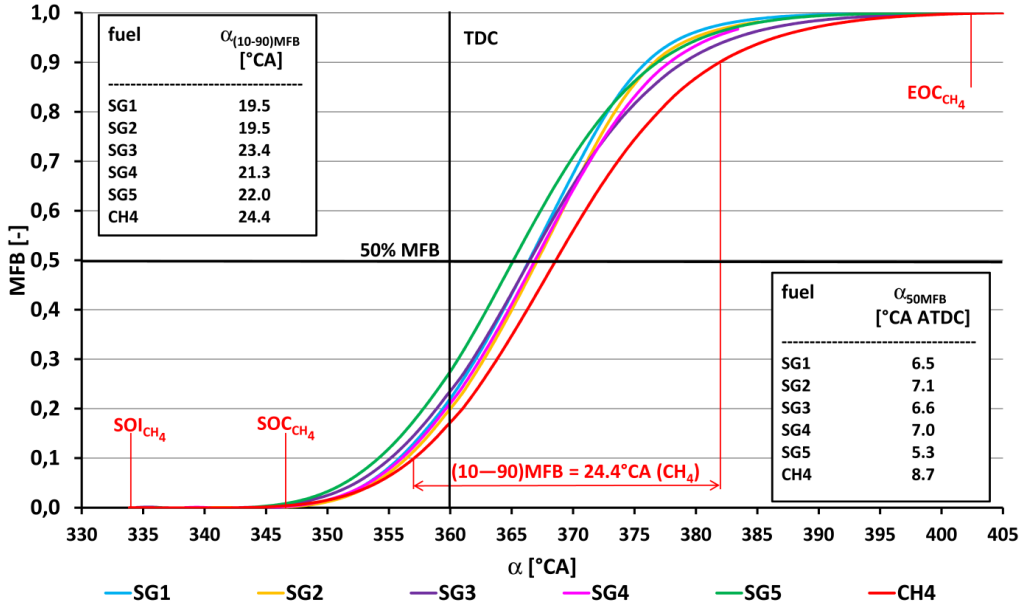

Fig. 5. Fuel combustion progress as a function of crankshaft angle for methane and syngas fuels (MFB - Mass Fraction Burned, α - Crankshaft Angle, SOC - Start of Combustion, SOI - Start of Ignition, TDC - Top Dead Center, EOC - End of Combustion); experimental conditions: engine speed 1500 min^{-1}, stoichiometric air-fuel ratio, full load, and optimal ignition timing for each gas

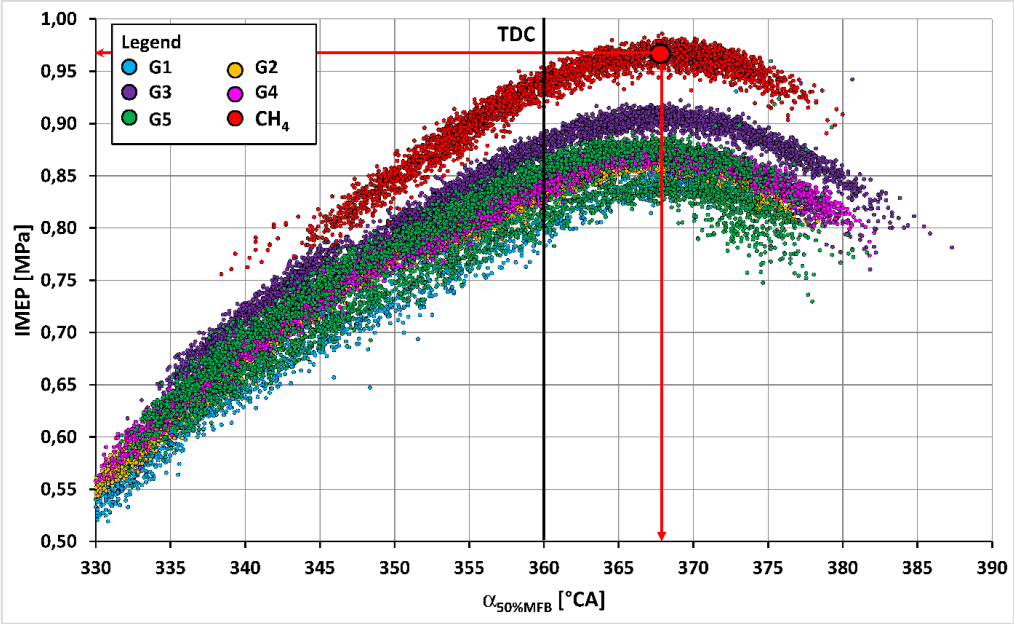

Fig. 6. Variation of the mean indicated effective pressure (IMEP) with crankshaft angle at the point where 50% of the fuel mass has been burned ($\alpha_{50\%MFB}$) for methane and syngas fuels; experimental conditions: engine speed 1500 min^{-1}, stoichiometric air-fuel mixture, full-load operation.

SG4 exhibited marginally higher performance parameters than SG2, reflected by an IMEP of 0.868 MPa and an output torque of 39.5 N·m, compared to 0.865 MPa and 38.7 N·m, respectively. This is despite SG2 having a slightly greater volumetric lower heating value (3.10 $MJ \cdot m^{-3}$ versus 3.09 $MJ \cdot m^{-3}$ for SG4). The observed deviation can be attributed to variations in the methane-to-carbon monoxide ratio between the two gaseous mixtures. When considered alongside the data in Table 1, these results confirm the expected positive correlation between the energy density per unit volume of a stoichiometric fuel mixture and the resulting indicated mean effective pressure and brake torque.

Figure 7 presents how the maximum in-cylinder pressure varies with the crankshaft position corresponding to 50% mass fraction burned (MFB 50%). The dataset was acquired by progressively advancing the ignition timing from 40°CA before TDC until reaching the operational stability limit of the engine. The adjustments were performed in fine steps of 1°CA, and each point in the plot represents the average of 197 successive cycles, ensuring statistical reliability.

For the baseline fuel, pure methane, the analysis indicates that the peak pressure plateaus at roughly 8.5 MPa. Once this threshold is reached, further ignition advance yields no tangible pressure gain. This behavior stems from the fact that, at excessive advance, the bulk of the combustion is completed during the late compression stroke, before the piston attains top dead center, meaning the trapped volume is still shrinking. Consequently, the work potential of the expanding gases after TDC is not significantly increased, even if peak pressure rises slightly earlier.

The pressure, MFB 50% relationship forms a reverse S-shaped trend, with a clear inflection at approximately 6.1 MPa and 8.5°CA after TDC. This point aligns with the most favorable operating condition for methane in this engine, corresponding to an ignition advance of about 26°CA before TDC.

The inverse S-curve behavior is characteristic of spark-ignition engines approaching their optimal phasing, where the trade-off between early combustion (which increases compression losses and knock tendency) and late combustion (which reduces effective expansion work) reaches a balance. The inflection point here is particularly important; it represents the crank angle at which half the mixture has burned under conditions that maximize both torque and efficiency. In practice, shifting MFB 50% closer to TDC can improve thermal efficiency but risks unstable combustion or detonation, while moving it too far after TDC sacrifices performance. The plateau in peak pressure beyond optimal timing suggests that for methane, further advance primarily increases negative work during compression, offering little benefit to net indicated efficiency.

Due to the 15% proportion of inert gases and the relatively low air-fuel ratio, a rise in hourly fuel consumption was observed. The consumption increased from 1.56 $kg \cdot h^{-1}$ for methane to 3.23 $kg \cdot h^{-1}$ for SG4, reaching a maximum of 3.87 $kg \cdot h^{-1}$ for SG2. As expected, this trend exhibited an inverse relationship with the air-fuel ratio.

4. CONCLUSION

The utilization of waste-derived gases in cogeneration applications presents a viable and environmentally advantageous alternative to conventional fossil fuels. Their adoption not only contributes to landfill waste reduction but also enhances the diversification of sustainable and low-carbon energy sources. When used in internal combustion engines, these gases can deliver operational characteristics comparable to those obtained with methane or natural gas.

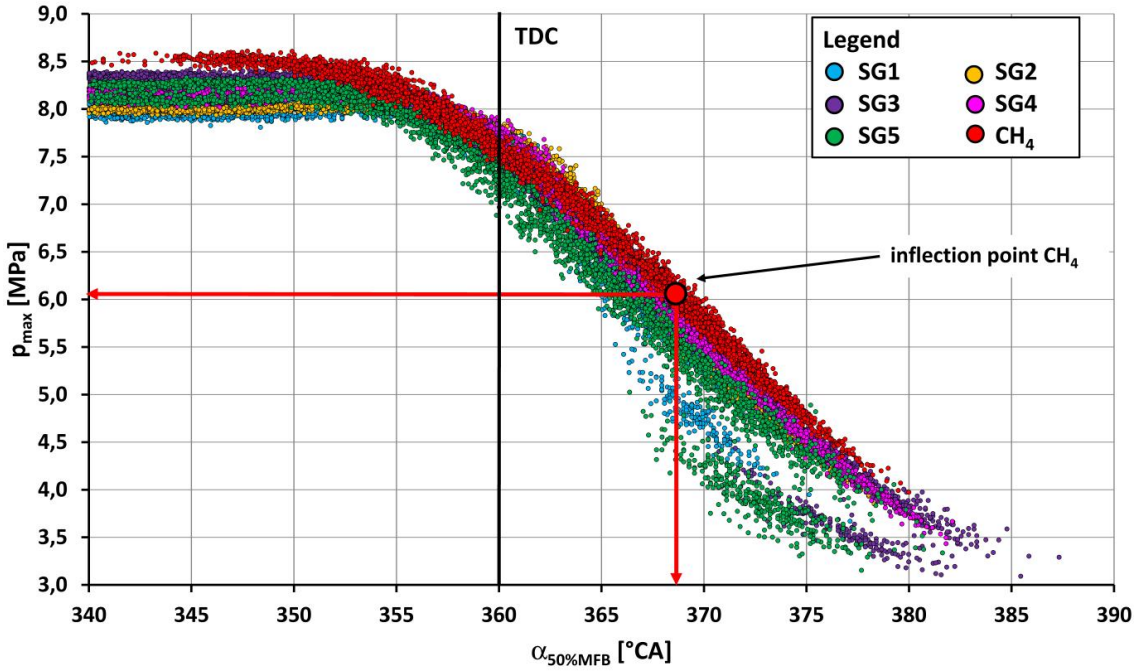

Fig. 7. Variation of the peak in-cylinder pressure with crankshaft position at the 50% mass fraction burned point for methane and syngas fuels (SG1-SG5). Experimental conditions: 1500 min^{-1}, stoichiometric air–fuel ratio, full load

Parameters such as peak in-cylinder pressure, its crank angle position, and the maximum pressure rise rate exhibited only minor deviations from methane-fueled operation. The most pronounced differences were observed in combustion duration and IMEP.

The inclusion of hydrogen within the fuel blend promoted faster combustion and shortened the overall burning period. However, due to the lower volumetric lower heating values (LHVs) of the syngas mixtures, a modest decline in engine torque was recorded. This reduction, accompanied by a slightly higher specific fuel consumption, remained limited to approximately 6-13.4%.

The principal effects resulting from variations in the gas mixture composition are summarized below:

- Variations in peak combustion pressure are primarily governed by the timing of the start of ignition (SOI) rather than the hydrogen fraction alone. For mixtures with higher hydrogen content, the SOI tends to shift closer to TDC, resulting in comparatively lower peak in-cylinder pressures.
- Higher hydrogen fractions consistently shortened the burn duration.
- Increased hydrogen content also lowered the maximum rate of pressure rise.
- For all mixtures except SG2 and SG4, the methane fraction primarily controlled the mixture's volumetric lower heating value at stoichiometry, exerting a direct effect on both the indicated mean effective pressure and the engine's torque output.
- Hourly fuel consumption rose as the air–fuel ratio decreased for all fuels.
- While most fuels operated stably, SG5 exhibited notable IMEP fluctuations, indicating potential operational instability.
- Comparing SG2 and SG3 shows that a higher CO-to-CH_4 ratio can accelerate combustion and produce higher peak pressures, though it slightly reduces overall engine performance.

It must be emphasized that the conclusions drawn from this investigation are valid for the examined steady-state operating regime only (1500 min^{-1}, full load, stoichiometric mixture). Under part-load conditions or lean combustion strategies, different relationships between hydrogen fraction, combustion duration, and IMEP could be expected due to altered thermodynamic and fluid-dynamic boundary conditions. Future research should therefore extend the experimental matrix to variable speed and load regimes to provide a more comprehensive characterization of high-energy syngas behavior in internal combustion engines.

These findings from the syngas evaluation can be applied in practical contexts, providing guidance for configuring waste gasification processes to optimize operational efficiency and enhance the economic performance of cogeneration systems.

Acknowledgement

This research was supported by the Slovak Research and Development Agency under Contract No. APVV-23-0456, APVV-20-0046, and was also supported by the Scientific Grant Agency under Contract No. VEGA 1/0666/24.

References

1. Grand View Research. *Waste To Energy Market Size, Share & Trends Report*, *2030*. Available at: https://www.grandviewresearch.com/industry-analysis/waste-to-energy-technology-industry.
2. Karmakar A., T. Daftari, K. Sivagami, et al. 2023. „A comprehensive insight into Waste to Energy conversion strategies in India and its associated air pollution hazard". *Environmental Technology & Innovation* 29. No 103017. DOI: 10.1016/j.eti.2022.103017.
3. Pio D.T., L.A.C. Tarelho. 2022. "Waste Gasification Technologies: A Brief Overview". *Clean Technologies* 1(1): 11-35. DOI: 10.3390/cleantechnol4010002.
4. EUROSTAT. *Municipal waste by waste management operations*. Available at: https://ec.europa.eu/eurostat/databrowser/view/env_wasmun.
5. Yang M., L. Chen, J. Wang, et al. 2023. "Circular economy strategies for combating climate change and other environmental issues". *Environmental Chemistry Letters* 21(1): 55-80. DOI: 10.1007/s10311-022-01497-3.
6. Vasileiadou A., L. Papadopoulou, et al. 2025. "Advancements in waste-to-energy (WtE) combustion technologies: A review of current trends and future developments". *Discover Applied Sciences* 7. No 457. DOI: 10.1007/s42452-025-06907-4.
7. Abedin T., J. Pasupuleti, J.K.S. Paw, et al. 2025. "From waste to worth: advances in energy recovery technologies for solid waste management". *Clean Techn Environ Policy* 27: 5963-5989. DOI: 10.1007/s10098-025-03204-x.
8. Nazari M., J. Haydary. 2024. "Gasification of municipal solid waste for power generation". *Journal of Chemistry and Chemical Engineering* 18(2): 45-58.
9. NETL. *Gasifiers for Waste*. Available at: https://www.netl.doe.gov/research/coal/energy-systems/gasification/gasifipedia/waste.

10. Suparmin P., R. Nurhasanah, L.O. Nelwan, et al. 2024. “Syngas for Internal Combustion Engines, Current State, and Future Prospects: A Systematic Review”. *International Journal of Automotive and Mechanical Engineering* 21(4): 11857-11876. DOI: 10.15282/ijame.21.4.2024.05.0920.
11. Costa M., D. Piazzullo. 2024. “The Effects of Syngas Composition on Engine Thermal Balance in a Biomass Powered CHP Unit: A 3D CFD Study”. *Energies* 17(3): 738. DOI: 10.3390/en17030738.
12. Fatiguso M., A.R. Valenti, S. Ravelli. 2024. “Comparative energy performance analysis of micro gas turbine and internal combustion engine in a cogeneration plant based on biomass gasification”. *Journal of Cleaner Production* 434: 139782. DOI: 10.1016/j.jclepro.2023.139782.
13. Caligiuri C., M. Renzi, D. Antolini, et al. 2023. „Optimizing the use of forestry biomass producer gas in dual fuel engines: A novel emissions reduction strategy for a micro-CHP system”. *Energy Conversion and Management* 20: 100498. DOI: 10.1016/j.ecmx.2023.100498.
14. Hagos F.Y., A.R.A. Aziz, S.A. Sulaiman. 2014. “Trends of Syngas as a Fuel in Internal Combustion Engines”. *Advances in Mechanical Engineering* 6. DOI: 10.1155/2014/401587.
15. Paykani A., et al. 2022. “Synthesis gas as a fuel for internal combustion engines in transportation”. *Progress in Energy and Combustion Science* 90: 100995. DOI: 10.1016/j.pecs.2021.100995.
16. Bonfanti N., P. Gaetani, G. Persico. 2020. “Internal combustion engines powered by syngas: A review”. *Energy Conversion and Management* 221: 113155. DOI: 10.1016/j.enconman.2020.113155.
17. Selvam D.C., Y. Devarajan, B. Nagappan, et al. 2025. “Sustainable fuel solutions: a comprehensive review of syngas in internal combustion engines”. *Chemical Papers* 79(7): 4019-4027. DOI: 10.1007/s11696-025-04069-6.
18. Kohn M.P., M.L. Basinger, M.J. Castaldi. 2011. “Performance of an Internal Combustion Engine Operating on Landfill Gas and the Effect of Syngas Addition”. *Industrial & Engineering Chemistry Research* 50(6): 3570-3579. DOI: 10.1021/ie101937p.
19. Quintero-Coronel D.A., A. Salazar, O.R. Pupo-Roncallo, et al. 2023. “Assessment of the interchangeability of coal-biomass syngas with natural gas for atmospheric burners and high-pressure combustion applications”. *Energy* 276: 127551. DOI: 10.1016/j.energy.2023.127551.
20. Kumar, A. 2023. “Experimental investigation of a dual stage ignition biomass downdraft gasifier for deriving the engine quality gas”. *Ain Shams Engineering Journal* 14(3): 101912. DOI: 10.1016/j.asej.2022.101912.

Received 28.10.2025; accepted in revised form 10.02.2026